Two Distinct Regions of the Yeast Mitochondrial ADP/ATP Carrier Are Photolabeled by a New ADP Analogue: 2-Azido-3′-*O*-naphthoyl-[β-^{32}P]ADP. Identification of the Binding Segments by Mass Spectrometry†

Anne-Christine Dianoux,*,‡ Florence Noël,‡ Christelle Fiore,‡,§ Véronique Trézéguet,|| Sylvie Kieffer,⊥ Michel Jaquinod,# Guy J.-M. Lauquin,|| and Gérard Brandolin‡

Laboratoire de Biophysique et Biochimie des Systèmes Intégrés, CNRS−UMR 5092, DBMS, CEA-Grenoble, 17 Rue des Martyrs, 38054 Grenoble Cedex 9, France, Laboratoire de Physiologie Moléculaire et Cellulaire, IBGC−CNRS, 1 Rue Camille Saint-Saëns, 33077 Bordeaux Cedex, France, Laboratoire de Chimie des Protéines, DBMS, CEA-Grenoble, 17 Rue des Martyrs, 38054 Grenoble Cedex 9, France, and Laboratoire de Spectrométrie de Masse des Protéines, IBS, 41 rue Jules Horowitz, 38027 Grenoble, France

Received March 17, 2000; Revised Manuscript Received July 5, 2000

ABSTRACT: A novel photoactivatable radioactive ADP derivative, namely, 2-azido-3′-*O*-naphthoyl-[β-^{32}P]-ADP (2-azido-N-[^{32}P]ADP), was synthesized with the aim at mapping the substrate binding site(s) of the yeast mitochondrial ADP/ATP carrier. It was used with mitochondria isolated from genetically modified strains of *Saccharomyces cerevisiae*, producing the native or the His-tagged Anc2p isoform of the carrier. In darkness, 2-azido-N-[^{32}P]ADP was reversibly bound to the carrier in mitochondria, without being transported. Upon photoirradiation, only the ADP/ATP carrier was covalently radiolabeled among all mitochondrial proteins. Specificity of labeling was demonstrated since carboxyatractyloside (CATR), a potent inhibitor of ADP/ATP transport, totally prevented the incorporation of the photoprobe. To localize the radioactive region(s), the purified photolabeled carrier was submitted to CNBr or hydroxylamine cleavage. The resulting fragments were characterized and identified by SDS−PAGE, Western blotting, amino acid sequencing, and MALDI-MS and ESI-MS analyses. Two short photolabeled distinct segments, eight and nine residues long, were identified: S183−R191, located in the central part of the ADP/ATP carrier; and I311−K318, belonging to its C-terminal end. Plausible models of organization of the nucleotide binding site(s) of the carrier involving the two regions specifically labeled by 2-azido-N-[^{32}P]ADP are proposed.

Understanding the mechanism of membrane transport proteins at the molecular level requires high-resolution structural information which will be collected from crystallization approaches and will allow elucidation of their three-dimensional structure. Besides, complementary knowledge of biophysical and biochemical properties of these proteins is required to understand their structure−function relationships. This includes identification and characterization of strategic domains involved in their functioning, mostly achieved by photolabeling approaches. Recent reports show that these techniques have been effective for identifying nucleotide binding regions within the polypeptide chain of membrane transport proteins (*1*−*4*). We have applied a similar method to map the substrate binding sites of the yeast *S. cerevisiae* mitochondrial ADP/ATP carrier protein, using a novel photochemical derivative of ADP.

The ADP/ATP carrier is a protein of the inner mitochondrial membrane, which in energized mitochondria exclusively catalyzes the 1-to-1 exchange of cytosolic ADP for ATP generated in the matrix space by oxidative phosphorylation. The ADP/ATP transport system can be blocked by very specific inhibitors, that bind to the carrier with high affinity and belong to two families: atractyloside (ATR) and carboxyatractyloside (CATR),[1] on the one hand, and bongkrekic acid (BA) and isobongkrekic acid (isoBA) on the other hand.

† This work was supported by the Commissariat à l'Energie Atomique, the Centre National de la Recherche Scientifique, the European Economic Community (fourth PCRD), the Région Rhône-Alpes, the Région Aquitaine, the University Joseph Fourier of Grenoble, and the University Victor Segalen of Bordeaux.

* Correspondence should be addressed to this author at the Laboratoire de Biophysique et Biochimie des Systèmes Intégrés, CNRS−UMR 5092, DBMS, CEA-Grenoble, 17 Rue des Martyrs, 38054 Grenoble Cedex 9, France. Phone number: (33) 476883173. Fax number: (33) 476885185. E-mail: acdianoux@cea.fr.

‡ Laboratoire de Biophysique et Biochimie des Systèmes Intégrés, CNRS−UMR 5092.

§ Present address: Department of Obstetrics/Gynecology & Reproductive Sciences, University of California San Francisco, 513 Parnassus Ave., San Francisco, CA 94143-0556.

|| Laboratoire de Physiologie Moléculaire et Cellulaire, IBGC−CNRS.

⊥ Laboratoire de Chimie des Protéines, DBMS.

Laboratoire de Spectrométrie de Masse des Protéines, IBS.

[1] Abbreviations: Anc2p, *S. cerevisiae* adenine nucleotide carrier, isoform 2; Anc2(His$_6$)p, His-tagged form of Anc2p; 2-azido-N-[^{32}P]-ADP, 2-azido-3′-*O*-naphthoyl-[β-^{32}P]ADP; 2-azido-N-AMP, 2-azido-3′-*O*-naphthoyl-AMP; CATR, carboxyatractyloside; DDM, dodecylmaltoside; EM, emulphogen; HTP, hydroxyapatite; CDI, *N*,*N*′-carbonyldiimidazole; SDS−PAGE, sodium dodecyl sulfate−polyacrylamide gel electrophoresis; MW, molecular weight; IMAC, immobilized metal ion affinity chromatography; MALDI-MS, matrix-assisted laser desorption ionization-mass spectrometry; ESI-MS, electrospray ionization-mass spectrometry; HPLC, high-pressure liquid chromatography; TLC, thin-layer chromatography.

10.1021/bi000618l CCC: $19.00
Published on Web 08/24/2000

Photolabeling of the ADP/ATP carrier inhibitor and substrate binding sites has been carried out with azido derivatives of ATR and ADP/ATP, respectively (*5, 6*). Concerning the nucleotide binding sites, conflicting results have been reported depending on the nature of the photoprobes and on the source of mitochondria. Dalbon et al. (*6*) identified two distinct domains of the ADP/ATP carrier of beef heart mitochondria specifically labeled by 2-azido-[α-^{32}P]ADP. The labeled peptides spanned residues C159−M200 and Y250−M281. On the other hand, Mayinger et al. (*7*) used 2-azido-[α-^{32}P]ATP and 8-azido-[γ-^{32}P]ATP to photolabel the ADP/ATP carrier in wild-type yeast *S. cerevisiae* mitochondria and found only one binding site located within the G172−M210 region.

In this paper we describe the synthesis of a novel nontransportable photoactivatable analogue of ADP, namely, 2-azido-3′-*O*-naphthoyl-[β-^{32}P]ADP (2-azido-N-[^{32}P]ADP), and its use to map the nucleotide binding site(s) of the membrane-embedded ADP/ATP carrier. Experiments were carried out with mitochondria from yeast cells producing Anc2p, the only isoform of the ADP/ATP carrier necessary for the cells to grow on a nonfermentable carbon source under aerobic conditions (*8*), and showed a specific photolabeling of the ADP/ATP carrier. Analyses of the fragments generated by chemical cleavages and tryptic digestion of photolabeled His-tagged Anc2p, Anc2(His$_6$)p, clearly demonstrated that two different restricted regions of the polypeptide chain were photolabeled by 2-azido-N-[^{32}P]ADP. They were identified by microsequencing, matrix-assisted laser desorption ionization-mass spectrometry, and electrospray-mass spectrometry (MALDI- and ESI-MS) analyses. Besides the central region S183−R191, a C-terminal region spanning residues I311−K318 also specifically bound 2-azido-N-[^{32}P]-ADP.

Results presented in this paper corroborate our previous statement of the existence of two regions of the ADP/ATP carrier involved in substrate recognition (*6*) and are discussed in terms of the participation of several nucleotide binding sites in the ADP/ATP transport process.

EXPERIMENTAL PROCEDURES

Materials

Chemicals. Dodecylmaltoside (DDM) was purchased from Calbiochem. Emulphogen BC 720 (EM) was obtained from GAF Corp. and was purified according to the procedure described by Ashani and Catravas (*9*). Hydroxyapatite (HTP) and poly(vinylidene difluoride) (PVDF) membranes were obtained from BioRad, and Ni−NTA (nitrilotriacetic acid) resin was from Qiagen. Ultrogel AcA 202 was obtained from Sepracore; Chelating Sepharose Fast Flow Cu−iminodiacetic acid resin (Cu−IDA resin), [^{32}P]H_3PO_4, and ECL reagent kit were purchased from Amersham Pharmacia.

Carboxyatractyloside (CATR), 2-chloroadenosine, cyanogen bromide (CNBr), *N*,*N*′-carbonyldiimidazole (CDI), sodium dodecyl sulfate (SDS), bovine serum albumin (BSA), dimethylformamide (DMF), hydroxylamine, imidazole, formic acid, diisopropyl fluorophosphate, and trifluoroacetic acid were obtained from Sigma/Aldrich. All other chemicals were of analytical grade.

Methods

Protein concentration was determined with the bicinchoninic acid (BCA) reagent kit from Sigma, using BSA as a standard.

Detergents and lipids were removed from protein fractions by overnight precipitation at −20 °C with 80% acetone and subsequent washings of the pellets with 20% trichloroacetic acid and diethyl ether. Proteins were then solubilized in formic acid for cleavage purposes or in sample dissociating buffer for SDS−PAGE.

Proteins obtained from purification steps and peptides resulting from chemical cleavages were separated by SDS−PAGE under the experimental conditions described either by Laemmli (*10*), using 5 and 13% acrylamide gels, or by Schägger and von Jagow (*11*), with 4, 10, and 20% acrylamide gels, depending on the MW range of the products to be analyzed. Gels were stained with Coomassie Brilliant Blue and analyzed for radioactivity with a PhosphorImager apparatus (Molecular Dynamics).

Proteins and peptides were electrotransferred onto PVDF membranes as described by Towbin et al. (*12*) and submitted either to automatic Edman degradation (ABI 492 Procise sequencer, Perkin-Elmer, Applied Biosystems Division) or to immunodetection. Anc2p, Anc2(His$_6$)p, and their derived fragments were immunodetected with antibodies raised in rabbits against either SDS-treated Anc2p carrier or 12- and 14-residue synthetic peptides corresponding to the N- and C-terminal sequences of Anc2p, respectively. The peptides and the corresponding antibodies were obtained as previously described (*13*). Alternatively, Anc2(His$_6$)p and derived fragments (see next section) were immunodetected with a monoclonal antibody directed toward a Penta-His sequence (Qiagen). The immune complexes were revealed with the ECL reagent kit from Amersham using peroxidase-linked to protein A or to anti-mouse IgG.

Yeast Strains and Media. Two genetically modified strains of the yeast *S. cerevisiae* were used: JL1-3-*ANC2*, which produced Anc2p; and JL1-3-*ANC2(His$_6$)*, producing a modified Anc2p isoform containing the extra sequence GSRSH-HHHHH at its C-terminal end [Anc2(His$_6$)p] (*14*). JL1-3-*ANC2* and JL1-3-*ANC2(His$_6$)* yeast cells were grown as described in (*8*).

Preparation of Yeast Mitochondria. Yeast cells were harvested during exponential growth phase when the OD 540 nm reached a value of 5.0. Mitochondria were prepared according to Daum et al. (*15*). Briefly, protoplasts obtained by enzymatic digestion of the cell wall with Zymolyase 20T (Seikagaku Corp.) were disrupted with a Dounce homogenizer in a medium made of 0.6 M mannitol, 0.1 mM EDTA, 10 mM Tris-HCl, 0.1% BSA, and 1 mM phenylmethylsulfonyl fluoride (PMSF), pH 7.4. Mitochondria were isolated by differential centrifugation and washed with the same medium but devoid of BSA and PMSF. They were used fresh or after storage in liquid nitrogen without significantly different results.

Purification of Anc2p and Anc2(His$_6$)p. All purification steps were carried out at 4 °C. Isolated yeast mitochondria were suspended at 10 mg of protein/mL in 0.1 M Na_2SO_4, 1 mM EDTA, 1 mM diisopropyl fluorophosphate, 10 mM Tris-HCl, pH 7.3, and solubilized by addition of 1% DDM and 1% EM. The soluble extract was submitted to HTP

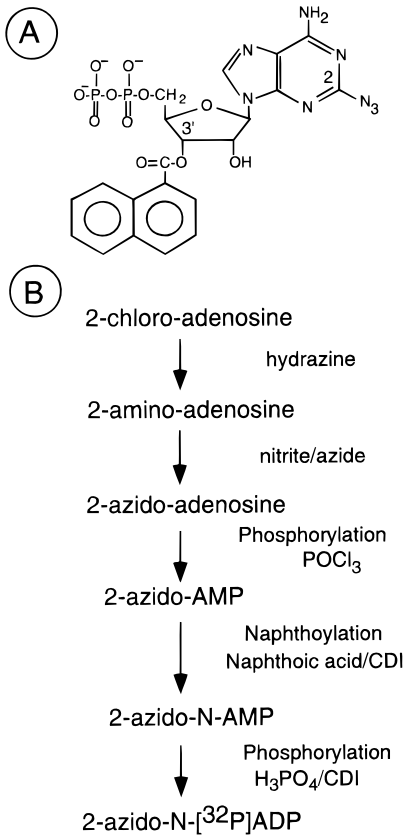

FIGURE 1: (A) Chemical structure and (B) schematic representation of synthesis steps of 2-azido-N-[^{32}P]ADP.

chromatography as described by Krämer and Klingenberg (*16*) with the modifications brought by Brandolin et al. (*8*). Partially purified Anc2p or Anc2(His$_6$)p was recovered in the flow-through fraction. Anc2(His$_6$)p was further purified by immobilized metal ion affinity chromatography (IMAC) using the Ni−NTA resin, following the experimental conditions established by Fiore et al. (*14*). Briefly, Anc2(His$_6$)p was bound to the resin in the presence of 5 mM $MgSO_4$, 50 mM NaP_i, pH 7.3, and 0.1% DDM. After extensive washing of the resin, it was eluted by 500 mM imidazole in 50 mM NaP_i, pH 7.3, with 0.1% DDM. Pure Anc2(His$_6$)p was then subjected to gel filtration on Ultrogel Aca 202, equilibrated in 0.1 mM EDTA, 50 mM Mops, pH 7.0, 0.1% DDM.

Synthesis and Characterization of 2-Azido-N-[^{32}P]ADP. The chemical structure and the synthesis of 2-azido-N-[^{32}P]-ADP are presented in Figure 1. All steps were carried out under inactinic light to prevent photolysis of the azido compounds. 2-Azido-AMP was synthesized as described by Boulay et al. (*17*). Briefly, the 2-chloroadenosine derivative was first converted to 2-aminoadenosine by hydrazine treatment and then to 2-azidoadenosine. The latter was phosphorylated using $POCl_3$ as described by Sowa and Ouchi (*18*).

Purified 2-azido-AMP was esterified by naphthoic acid following the procedure described by Schäfer and Onur (*19*), based on the use of the imidazolide derivative of 1-naphthoic acid (*20*). All steps were performed in siliconized glassware to avoid adsorption of compounds due to their marked hydrophobic character. 2-Azido-N-AMP was purified by HPLC on a C18 RP column eluted for 30 min with a linear ethanol gradient from 0 to 100% in 0.1% acetic acid and 1 mM ammonium acetate, pH 6.0, at a flow rate of 1 mL/min. Under these conditions, 2-azido-N-AMP and unreacted naphthoic acid were eluted with retention times of 19 and 20.2 min, respectively, far away from 2-azido-AMP (12 min). The purity of 2-azido-N-AMP was checked by ascending thin-layer chromatography (TLC) on a cellulose-coated plastic sheet (F1440, from Schleicher & Schuell). The chromatogram was developed in a solvent mixture made of butanol/acetic acid/water (5:2:3, v/v/v) for 6 h. 2-Azido-N-AMP migrated as a single dark blue fluorescent spot with an R_f value of 0.8 (data not shown).

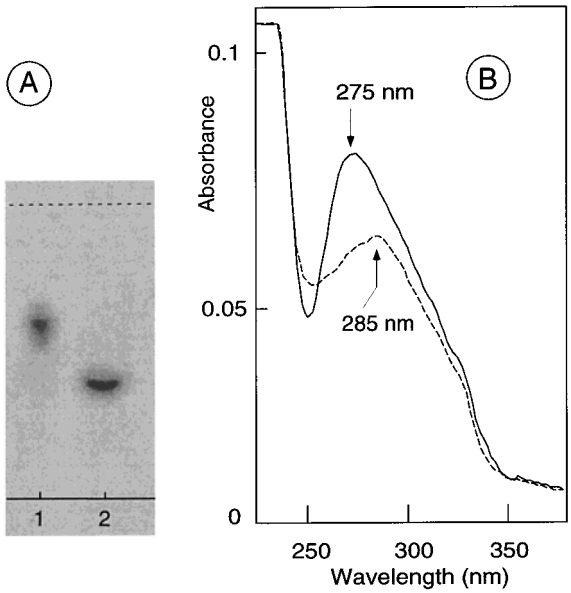

FIGURE 2: Characterization of 2-azido-N-[^{32}P]ADP. (A) Control of purity by autoradiography after TLC on a cellulose plate developed in butanol/acetic acid/water (5/2/3, v/v/v). Lane 1, 2-azido-N-[^{32}P]ADP; lane 2, [^{32}P]phosphate. (B) Absorption spectra of 2-azido-N-[^{32}P]ADP (5 μM in 0.1 N HCl) before (—) and after UV irradiation (- - -) (see Experimental Procedures).

Phosphorylation of 2-azido-N-AMP to 2-azido-N-[^{32}P]-ADP was performed in anhydrous DMF as described by Hoard and Ott (*21*). Briefly, the P_i group of 2-azido-N-AMP was first activated with CDI in anhydrous DMF, and the resulting imidazolide was reacted with tributylammonium [^{32}P]phosphate (specific radioactivity between 500 and 1000 cpm/pmol) for 16 h at room temperature. 2-Azido-N-[^{32}P]-ADP was purified by TLC under the experimental conditions described for 2-azido-N-AMP; it was detected by autoradiography as a single spot (R_f of 0.6) and separated from unreacted [^{32}P]phosphate (R_f of 0.4) (Figure 2A). The corresponding cellulose strips were cut off and eluted with 50% ethanol. The recovered 2-azido-N-[^{32}P]ADP was dried under vacuum and resolubilized in the appropriate buffer for labeling experiments.

The identity of the purified product as 2-azido-N-[^{32}P]ADP was ascertained by MALDI-MS. The spectrum displayed three characteristic peaks corresponding to 2-azido-N-[^{32}P]-ADP, *m*/*z* 623, and to degraded forms resulting from laser irradiation, in which either the azido group or the azido group plus the β-phosphate group of ADP have been degraded, *m*/*z* 597 and 517, respectively. The last species was the best desorbed (data not shown). The absorbance spectrum of 2-azido-N-[^{32}P]ADP in 0.1 N HCl (Figure 2B) showed a maximum at 275 nm. Photodegradation of the azido group by UV light irradiation of the sample (2 min exposure to

254 or 312 nm UV light, 180 W lamp, UV Products) resulted in a significant absorbance intensity decrease of the peak and a shift of the maximum to 285 nm (Figure 2B). This absorbance maximum markedly differs from that of photoirradiated 2-azido-ADP (254 nm), being red-shifted because of the UV-insensitive absorbance of the naphthoyl moiety at 300 nm. The concentration of 2-azido-N-[^{32}P]ADP was measured based on a molecular extinction coefficient of 15 200 M^{-1} cm^{-1} at 275 nm in 0.1 N HCl (*6*).

Reversible Binding of 2-Azido-N-[^{32}P]ADP to Mitochondria. Binding assays of 2-azido-N-[^{32}P]ADP (500−1000 cpm/pmol) to freshly isolated or to liquid nitrogen stored mitochondria were carried out at 4 °C in the dark, using siliconized glassware. Mitochondria were suspended at a concentration of 2.5 mg of protein/mL in a medium made of 0.12 M KCl, 1 mM EDTA, 10 mM Tris-HCl, pH 7.3, in the presence of increasing concentrations of 2-azido-N-[^{32}P]-ADP up to 22 μM and allowed to incubate for 1 h (control experiment). Two other parallel series of incubation were run in the presence of 20 μM CATR: in the first one, CATR was added 1 h after 2-azido-N-[^{32}P]ADP addition, and the suspension was allowed to incubate for a further 10 min period. In the second one, CATR was added to the mitochondrial suspension 10 min prior to 2-azido-N-[^{32}P]ADP addition, and the incubation was continued for 1 h. Mitochondria were centrifuged, and the radioactivity associated with the pellets was determined by scintillation counting after solubilization with 5% Triton X-100, 0.5 M NaCl in 0.1 M Tris buffer, pH 7.3. The difference between the radioactivity incorporated into mitochondria in the control experiment and in the experiment in which CATR was added after 2-azido-N-[^{32}P]ADP was ascribed to specific binding of the probe. Had transport occurred, a difference would be observed between the inhibition curves obtained when CATR was added prior to or after 2-azido-N-[^{32}P]ADP.

Covalent Photolabeling of the ADP/ATP Carrier by 2-Azido-N-[^{32}P]ADP in Mitochondria. Mitochondria (10 mg of protein/mL) were incubated for 30 min at 4 °C in the dark with 20 μM 2-azido-N-[^{32}P]ADP, in the presence or absence of 20 μM CATR, as described for reversible binding assays (see above). Then, samples were placed in Petri dishes over crushed ice and photoirradiated for 2 min with UV light (254 or 312 nm 180 W lamp from UV Products) placed at 10 cm above the surface medium. The mitochondria were spun down and washed twice with cold incubation buffer to remove unbound probe. As controls, aliquots of the mitochondrial suspensions were solubilized in SDS dissociating buffer and analyzed by SDS−PAGE, according to Laemmli (*10*). Covalently incorporated ^{32}P radioactivity in proteins was detected either from stained or from unstained gels with a PhosphorImager apparatus.

2-Azido-N-[^{32}P]ADP-photolabeled Anc2p or Anc2(His$_6$)p were then purified as described above.

Chemical Cleavage of the ADP/ATP Carrier. Cleavage of Anc2(His$_6$)p at the N171−G172 peptide bond was carried out with hydroxylamine in aqueous solution (*22*). An HTP pass-through fraction containing partially purified ^{32}P-photolabeled Anc2(His$_6$)p in 0.2% EM was incubated with 2 M hydroxylamine in 0.1 M Na_2CO_3, pH 9.0, for 4 h at 37 °C. Detergents and lipids were removed as previously described; then the resulting products were analyzed after SDS−PAGE (*10*).

Cleavage of Anc2p or Anc2(His$_6$)p at Met residues was performed with CNBr (*23*). The isolated ^{32}P-photolabeled carrier samples, devoid of lipids, detergents and salts (see Methods under Experimental Procedures), were solubilized at a concentration of 10 mg of protein/mL in 70% formic acid and treated with a 500-fold molar excess of CNBr over the Met content. The reaction was allowed to proceed for 40 h at 37 °C in the dark, and then was ended by addition of 5 volumes of distilled water and freeze-dried. The released peptides were separated by SDS−PAGE (*11*), and their radioactivity was detected; they were further analyzed by amino acid sequencing, Western blotting, and MALDI- and ESI-MS.

MALDI- and ESI-MS Analyses. MALDI mass spectra were recorded using either a Bruker Biflex spectrometer (Bruker-Franzen, Bremen, Germany) or a Voyager Elite spectrometer (Perspective Biosystems, Framingham, MA). For analysis, 1 μL of each sample was mixed with 1 μL of a saturated solution of 2,5-dihydroxybenzoic acid (DHB) in 60% acetonitrile containing 0.1% trifluoroacetic acid. The protein concentration in samples containing salts and detergent was adjusted to obtain the best detection sensitivity. Spectra were calibrated either with autodigested trypsin peptides or, externally, with monomeric forms of BSA and horse myoglobin, depending on the explored MW range.

For in-gel enzymatic digestion (*24*), Coomassie Blue stained bands of the SDS−PAGE gel corresponding to proteins or peptides were excised and successively washed with 25 mM NH_4HCO_3, 25 mM NH_4HCO_3 in 50% acetonitrile and 25 mM NH_4HCO_3, before drying in a vacuum centrifuge. Gel fragments were reswollen in 25 mM NH_4HCO_3 containing 0.5 μg of trypsin (sequencing grade, Promega) and incubated for 24 h at 37 °C. MALDI-MS analyses were carried out on a mixture of a 0.4 μL sample of the digest solution and 0.5 μL of a saturated solution of α-cyano-4-hydroxy-*trans*-cinnamic acid in 40% acetonitrile and 0.1% trifluoroacetic acid.

ESI mass spectra were recorded on a API III PE-SCIEX spectrometer (Halifax, Canada). Prior to analyses, the CNBr peptides were purified by HPLC on a C18-RP column eluted at 1 mL/min for 30 min with a linear acetonitrile gradient from 0 to 100% in 0.1% trifluoroacetic acid. The recovered fractions were directly injected into the spectrometer.

RESULTS

Synthesis and Characterization of 2-Azido-N-[^{32}P]ADP. The main features of synthesis, control of purity (TLC), and physicochemical characterization (MALDI analyses and absorption spectra) of 2-azido-N-[^{32}P]ADP are described under Experimental Procedures.

The yield of synthesis of 2-azido-N-[^{32}P]ADP was mainly limited by (1) the coupling efficiency of the naphthoyl group to 2-azido-AMP, a critical step which required strict anhydrous conditions and high-quality CDI, (2) the difficulties arising from the separation of 2-azido-N-AMP from naphthoic acid, due to their similar chromatographic behavior, and (3) the hydrophobic character of 2-azido-N-AMP, requiring the use of siliconized glassware. Several attempts were made to improve the separation of these two compounds, including HPLC with several types of derivatized silica beads (RP-C18, -C8, -C4, or -CN) under appropriate

elution conditions, TLC, or paper chromatography using different solvent systems. Optimization of purification procedures led to the HPLC experimental conditions described under Experimental Procedures.

Due to the short half-life of ^{32}P, the last step of synthesis of 2-azido-N-[^{32}P]ADP, namely, phosphorylation of 2-azido-N-AMP with [^{32}P]phosphate, was carried out, when required, from stored 2-azido-N-AMP. As this intermediate compound was very stable, it could be kept for several weeks as a concentrated aqueous solution at −20 °C. The synthesized 2-azido-N-[^{32}P]ADP was directly used for labeling experiments and showed no significant degradation during CNBr cleavage assays.

2-Azido-ADP analogues are particularly suitable to properly identify the specific substrate binding sites of the ADP/ATP carrier by photolabeling, because of two main features: (1) the azido group, which is responsible for covalent incorporation of the probe, is attached to the adenine moiety without a spacer arm, thus allowing specific covalent labeling of the recognition site of the carrier upon photoirradiation; and (2) 2-azido-ADP is stabilized in the "anti" conformation, which is best recognized by the carrier (*25*). A further modification of ADP, namely, addition of a naphthoyl group on the ribose moiety of adenosine, was introduced to increase the stability of the probe. We have established, from control experiments, that either 2-azido-ADP or 2-azido-ATP, when incubated with yeast mitochondria, underwent rapid degradation to azidoadenosine and to a lower extent to azidoadenine even at 4 °C (data not shown). This effect could be totally prevented when using 2-azido-N-[^{32}P]ADP. Both ADP and ATP are high-affinity substrates for the carrier, but the synthesis of an ADP vs ATP derivative was favored, due to its lower use as a substrate for various enzymes, such as kinases.

As shown thereafter, the presence of azido and naphthoyl groups does not impair the specific recognition and binding properties of 2-azido-N-[^{32}P]ADP to the ADP/ATP carrier.

Reversible Binding of 2-Azido-N-[^{32}P]ADP to the ADP/ATP Carrier in Mitochondria. The number and affinity of binding sites for 2-azido-N-[^{32}P]ADP of the membrane-embedded ADP/ATP carrier were determined on mitochondria from yeast strains producing Anc2p or Anc2(His_6)p. Mitochondria were incubated in the presence of increasing concentrations of 2-azido-N-[^{32}P]ADP as described under Experimental Procedures. The numbers of specific binding sites were found similar for mitochondria from both yeast strains, between 370 and 470 pmol/mg of protein. Such values are comparable to that found for [^{3}H]atractyloside binding sites under the same experimental conditions (data not shown). The dissociation constant ($K_d \sim 3.3$ μM) was very close to that found for the binding of N-ADP (*26*). Similar results were obtained when CATR was added prior to or after 2-azido-N-[^{32}P]ADP, indicating that this substrate analogue was not transported. These findings corroborate previous results according to which addition of either azido or naphthoyl groups to ADP or ATP resulted in derivatives that were nontransportable, but still specifically recognized and bound with high affinity by the ADP/ATP carrier (*6*, *26*).

Covalent Photolabeling of the ADP/ATP Carrier by 2-Azido-N-[^{32}P]ADP in Mitochondria. Mitochondria from yeast strains producing Anc2p or Anc2(His_6)p were incubated with 2-azido-N-[^{32}P]ADP in the absence or presence of CATR and then covalently photolabeled. After solubilization, mitochondrial proteins were separated by SDS−PAGE (Figure 3) and detected by Coomassie Blue staining (panel A) and ^{32}P radioactivity (panel B). Similar results were obtained from both types of mitochondria. Among numerous proteins detected in crude lysates, ^{32}P radioactivity is exclusively associated with a protein band of apparent MW 35 000. Preincubation of mitochondria with 20 μM CATR, which displaces nucleotides bound to the carrier, totally abolishes the photolabeling (panel B, lane b). This result demonstrates that the 35 kDa protein specifically photolabeled by 2-azido-N-[^{32}P]ADP is most probably the ADP/ATP carrier.

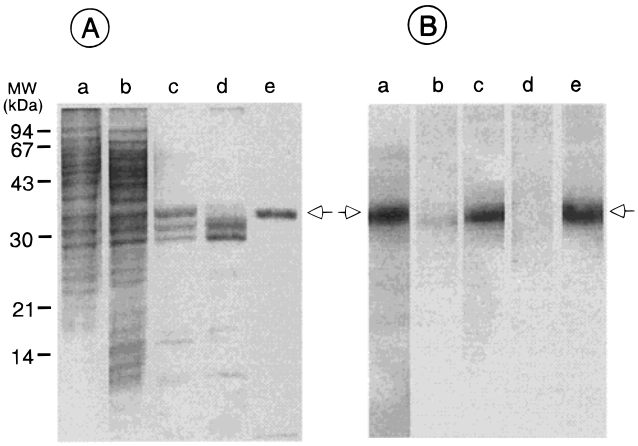

FIGURE 3: Separation by SDS−PAGE according to (*10*) of proteins from JL1-3-*ANC2(His$_6$)* yeast mitochondria photolabeled with 2-azido-N-[^{32}P]ADP. (A) Coomassie Blue staining. (B) ^{32}P radioactivity. Lanes a and b: crude lysates from mitochondria labeled in the absence (a) or presence (b) of 20 μM CATR. Lanes c: HTP pass-through fraction. Lanes d and e: unbound and imidazole-eluted fractions from Ni−NTA chromatography, respectively. Open arrows point to Anc2(His_6)p. MW of standard proteins are indicated.

To ensure this statement, analyses were carried out after isolation of the ADP/ATP carrier from mitochondria photolabeled with 2-azido-N-[^{32}P]ADP. The enriched fraction obtained after HTP chromatography showed that only one protein band, out of the three detected by Coomassie Blue staining (Figure 3, panel A, lane c) and migrating in the 35 kDa region, was photolabeled by 2-azido-N-[^{32}P]ADP (panel B, lane c). It was clearly identified as the ADP/ATP carrier by Western blotting using anti-Anc2p antibodies; the two other mitochondrial proteins corresponded to the phosphate carrier and the porin (*14*). Because of the presence of these contaminant proteins and of large amount of ergosterol (*27*), the HTP-purified carrier was not suitable for accurate mapping of the substrate binding sites. Instead, for this purpose, we used the Anc2(His_6)p which was further purified by IMAC (*14*). It migrated as a single Coomassie Blue stained radioactive band, as illustrated in Figure 3 (panels A and B, lanes e). Unlabeled porin and phosphate carrier were recovered in the flow-through fraction of the Ni−NTA column (Figure 3, panels A and B, lanes d).

Fragmentation of the photolabeled carrier and identification of the ADP binding region(s) were thus mainly carried out with purified Anc2(His_6)p.

Localization of the 2-Azido-N-[^{32}P]ADP-Photolabeled Region(s) of Anc2(His$_6$)p. Photolabeled-Anc2(His_6)p was

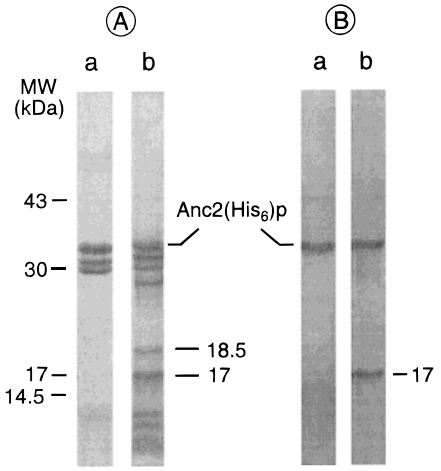

FIGURE 4: Separation by SDS−PAGE according to (*10*) of peptides released by hydroxylamine cleavage of 2-azido-N-[^{32}P]ADP-photolabeled Anc2(His$_6$)p. Cleavage was carried out with the HTP pass-through fraction. (A) Coomassie Blue staining. (B) ^{32}P radioactivity. Lanes a: control. Lanes b: after hydroxylamine treatment. The 17 and 18.5 kDa peptides indicated are those released from Anc2(His$_6$)p by hydroxylamine cleavage.

subjected to fragmentation with two different chemical reagents, hydroxylamine or CNBr, under the experimental conditions described under Experimental Procedures. The number, identity, and MW values of the peptides of Anc2-(His$_6$)p specifically released by cleavage with either of these two reagents were predicted from the amino acid sequence deduced from the *ANC2* DNA sequence (GenBank/EMBL Data Bank, accession number X74427), and taking into account the His-tag extension.

A rough localization of the photolabeled region(s) was first carried out after hydroxylamine cleavage of the carrier at the N171−G172 bond, which released two peptides (17 000 and 18 500 MW). It was performed with an HTP pass-through fraction containing the 2-azido-N-[^{32}P]ADP-labeled Anc2(His$_6$)p, and the resulting fragments were analyzed by SDS−PAGE (Figure 4). Though Coomassie Blue staining revealed the presence of several peptides released from the ADP/ATP carrier, the phosphate carrier, and the porin (Figure 4, panel A), the ^{32}P radioactivity was found associated only with the 17 kDa peptide (Figure 4, panel B, lane b). From the distribution of radioactivity in the 17 kDa band and in the nondigested Anc2p band, the yield of cleavage was evaluated to 40%. Identity of the 17 kDa peptide to the C-terminal part of Anc2(His$_6$)p was confirmed by immunodetection with antibodies raised against the C-terminal sequence of Anc2p (data not shown). As a consequence, 2-azido-N-[^{32}P]ADP is bound to the region of Anc2(His$_6$)p comprised between residues G172 and H328.

CNBr cleavage at Met residues of 2-azido-N-[^{32}P]ADP-labeled Anc2(His$_6$)p after IMAC purification was very efficient, leading to almost 100% yield. Eight peptides are predicted to be released. They are named CB1 to CB8 according to their position within the Anc2(His$_6$)p sequence from the N- to the C-terminus. They are listed in Table 1, with both their theoretical masses and their average masses (*m*/*z*) measured by MALDI- and/or ESI-MS after conversion of the C-terminal Met to homoserine (Hse) (see later).

As shown in Figure 5, SDS−PAGE allowed separation of the CNBr peptides into several Coomassie Blue stained

Table 1: Characteristics of the Peptides Generated from CNBr Cleavage of Anc2(His$_6$)p

	localization in Anc2(His$_6$)p sequence[a]	theoretical average mass (Da)	measured average mass (*m*/*z*)[e]	
			MALDI-MS	ESI-MS
CB1	S2−Hse29	3011.6	3054[b]	3053.1
CB2	G30−Hse57	2867.2	2868	2866.2
CB3	L58−Hse114	6513.5	6522	nd[d]
CB4	F115−Hse210	10285.8	10284	nd
CB5[c]	Y211−Hse255	4893.6	4894	nd
CB6[c]	T258−Hse304	4629.3	4632	nd
CB7	Y305−Hse310	766.8	nd	766.4
CB8	I311−H328	2190.5	2191	2190.2

[a] Met at the C-terminus was converted to homoserine (Hse) (see text). [b] This value includes the presence of an acetyl group on Ser2 (see text). [c] The gap between the sequences of the CB5 and CB6 peptides is due to the presence of three Met residues at positions 255, 256, and 257. [d] nd: not determined. [e] Standard deviation is less than 0.2% for MALDI mass determination, except for CB3 (∼1%; see text), and is less than 0.05% for ESI mass determination.

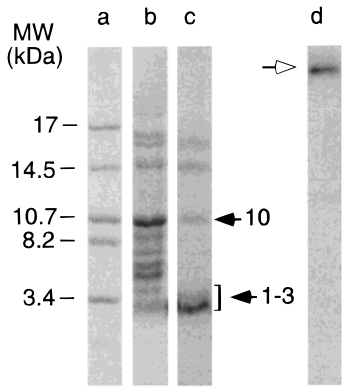

FIGURE 5: Separation by SDS−PAGE according to (*11*) of peptides resulting from CNBr cleavage. Anc2(His$_6$)p was photolabeled by 2-azido-N-[^{32}P]ADP, purified by IMAC, and then cleaved by CNBr. Coomassie Blue staining of standard MW markers (lane a) and of CNBr-released peptides (lane b). Lane c: ^{32}P radioactivity associated with CNBr peptides. Black arrows point to the 10 000 and 1000−3000 MW labeled regions. Lane d: ^{32}P radioactivity associated with the IMAC-purified labeled Anc2(His$_6$)p (open arrow).

bands with apparent MW ranging from 16 000 to 1000−3000 (lane b) as compared to standard MW proteins (lane a). Peptides were identified by direct automatic Edman degradation analysis and by immunodetection, after electrotransfer onto a PVDF membrane. Four photolabeled peptides, bearing different amounts of radioactivity, were detected with apparent MW of 16 000, 14 000, 10 000, and 1000−3000 (Figure 5, lane c). The 10 kDa band corresponded to only one peptide, CB4, as assessed by identification of its N-terminal amino acid sequence FG-FKKE. The presence in this band of other peptides, with a blocked N-terminal residue (see later), could be excluded, as no incomplete CNBr cleavage could generate peptides of similar MW. It can be concluded that CB4 is one of the peptides labeled by 2-azido-N-[^{32}P]ADP.

From microsequencing, it was found that the 16 and 14 kDa weak radioactive bands corresponded to CB3+CB4 and CB4+CB5, respectively, resulting from incomplete CNBr cleavage of the carrier. Their radioactivity was due to the presence of CB4, since CB3 and CB5 were not radioactive.

Therefore, the specific ^{32}P labeling was restricted to CB4 and to fragments migrating with apparent MW of 1000−

3000 (Figure 5, lane c, marked with arrows). The same conclusions were drawn from similar experiments carried out with purified Anc2p, thus demonstrating that the His-tag extra sequence was not involved per se in the photoprobe binding. However, the presence of a large amount of ergosterol in samples containing the CNBr-cleaved Anc2p precluded further analyses of the low MW peptides.

Four peptides are expected to migrate in the 1000−3000 MW region (Table 1). Edman degradation analysis revealed the presence in unequal amounts of three peptide sequences. They were assigned to peptides CB2 (GGVSAAVAKT), CB7 (YDQLQ), and CB8 (ILFGKKFKGSRSH) (see Table 1). Although 10 sequencing steps were carried out, no occurrence of the peptide made of CB7 (6 residues long) + CB8, that would have resulted from a partial CNBr cleavage, was detected. In addition, the presence of peptide CB1, spanning residues 2−29, in the 1000−3000 MW region of the gel, was demonstrated by immunodetection with specific anti-N-terminus Anc2p antibodies. CB1 peptide could not be sequenced, due to the presence of an N-terminal blocking group (see later). In conclusion, one or several of these peptides do carry the photoprobe.

As stated above from hydroxylamine cleavage, the photolabeling of Anc2(His_6)p was localized only to the C-terminal part of the carrier, i.e., to the region extending from residues G172 to H328. Thus, peptides CB1 and CB2, which are located close to the N-terminal end of Anc2(His_6)p, can be safely excluded as potential targets of photolabeling. Therefore, the potential photolabeling sites were restricted to peptides CB7 and/or CB8, located in the C-terminal end of Anc2(His_6)p.

This result was confirmed by an immunodetection experiment based on the presence of the His-tag extension at the C-terminal end of Anc2(His_6)p. The whole mixture of ^{32}P-labeled CNBr peptides was solubilized in 0.1% DDM and subjected to IMAC on Cu−IDA resin, which is able to bind efficiently His-tagged peptides (*28*). Bound material eluted from the Cu−IDA resin with 30 mM EDTA, pH 7.0, strongly immunoreacted in dot blot assays with a monoclonal anti-Penta-His antibody whereas the unbound peptides were unreactive. As expected, the EDTA-eluted peptide was radiolabeled and migrated in the 1000−3000 MW region during SDS−PAGE (data not shown). This result confirmed that 2-azido-N-[^{32}P]ADP was covalently bound to the C-terminal peptide CB8 and/or, still possible but most unlikely, to peptide CB7. In addition, since the low MW peptides generated from CNBr cleavage of photolabeled Anc2p (non-His-tagged isoform, ending at K318) were also ^{32}P-labeled, binding of the probe can be restricted to the C-terminal fragment ending at position 318.

MALDI- and ESI-MS Analyses of the CNBr Peptides. MALDI-MS analysis of the whole peptide mixture released by CNBr treatment of Anc2(His_6)p led to discrimination of the predicted peptides, according to their expected masses (Table 1). Only the shortest peptide, CB7, was not detected, as the spectra were scanned in the mass range between 800 and 12 000 Da. The large peptide CB4, *m*/*z* 10 284, appeared as a low-resolution broad peak. Unexpectedly, CB3 displayed numerous peaks in the 6000−6500 *m*/*z* range. In addition, it migrated as two distinct peptides in SDS−PAGE, that is discussed later. CB5 and CB6 peptides appeared as split peaks, due to random CNBr cleavage at each Met residue of the MMM sequence between them (data not shown).

ESI-MS, carried out on HPLC-separated CNBr peptides from Anc2(His_6)p (see Experimental Procedures), allowed identification of the four short peptides, including CB7 (Table 1), which comigrated during SDS−PAGE (Figure 5).

The experimental conditions for CNBr cleavage, 70% formic acid for 40 h, led to unintended random O-formylation mainly on Ser and Thr residues. This chemical modification results in the splitting of CNBr peptides into several peaks, because of mass implementation (+28 per formyl group) related to the number of modified Ser/Thr residues. The formylation extent was time-dependent, and the reaction proceeded even at −18 °C. In attempts to avoid this side effect, formic acid was replaced with trifluoroacetic acid or acetic acid, but CNBr cleavage did not occur under these conditions, probably due to the loss of solubility of Anc2-(His_6)p. On the other hand, treatment of the CNBr peptide mixture with 50 mM NH_4HCO_3, pH 9.0, for 15 min at 95 °C (*29*) led to a significantly decreased, though incomplete, deformylation. In addition, those alkaline conditions favored the homoserine (Hse) form over the Hse-lactone form of the cleaved Met.

Refinement of the 2-Azido-N-[^{32}P]ADP Binding Regions. MS analyses were applied to confirm the occurrence of two 2-azido-N-[^{32}P]ADP-labeled segments and to sharpen their localization within CB4 and the C-terminal region of Anc2-(His_6)p.

Attempts to detect photolabeled CB4 by MALDI-MS were unsuccessful. Several hypotheses could account for this observation: (a) the low resolution of MALDI-MS in this MW range and the formylation side-reaction, as exposed in the preceding section; (b) the low desorption of the labeled fragment as compared to the unlabeled one; (c) the low yield of covalent binding of the probe to the carrier.

A more precise assignment of bound 2-azido-N-[^{32}P]ADP to the restricted region of CB4 could be achieved when comparing MALDI-MS analyses of photolabeled and unlabeled samples after in-gel trypsin digestion (Figure 6). In panel A, the MALDI mass spectrum from ^{32}P-labeled CB4 shows the presence of an additional fragment, *m*/*z* 1447, as compared to the control (Figure 6, panel B). This value can only match with the peptide S183−R191, *m*/*z* 937, bearing the covalently bound 2-azido-N-[^{32}P]ADP. This result is in agreement with the labeling of the C-terminal fragment, G172−H328, arising from hydroxylamine treatment of Anc2-(His_6)p as described earlier.

We have shown that the CB8 peptide, out of the pool of CB1, CB2, CB7, and CB8, which comigrated during SDS−PAGE, was very likely photolabeled by 2-azido-N-[^{32}P]ADP. This result was clearly confirmed by MALDI-MS comparative analysis of the CNBr-released peptides of either labeled or unlabeled Anc2(His_6)p (Figure 6, panels C and D). Profiles were identical for both samples, except for the presence of one additional fragment, *m*/*z* 2743, detected in the photolabeled sample. It most probably corresponds to CB8 (residues I311−H328, 2189 Da), the mass of which was incremented by bound 2-azido-N-[^{32}P]ADP and a K^+ cation.

In summary, two binding regions for 2-azido-N-[^{32}P]ADP on Anc2(His_6)p have been precisely assigned: one located in the central region of the polypeptide chain, extending from S183 to R191 (SDGVAGLYR); and the other at the

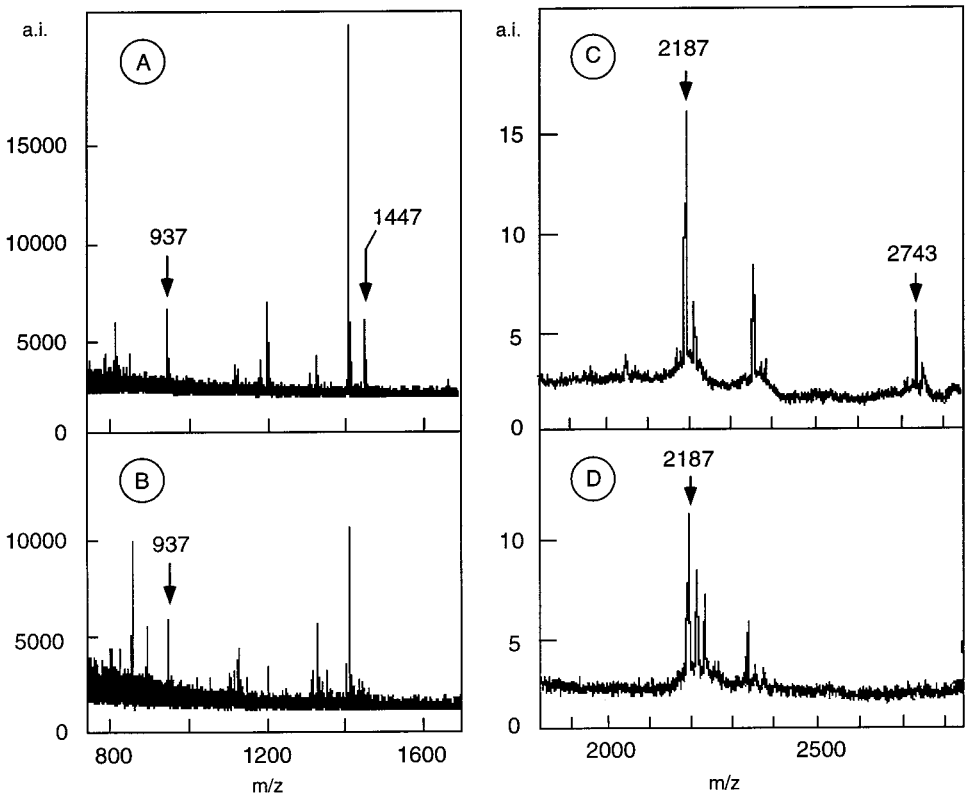

FIGURE 6: MALDI mass spectra of Anc2(His$_6$)p fragments covalently photolabeled by 2-azido-N-[^{32}P]ADP. Comparison of tryptic digests of (A) labeled or (B) unlabeled CB4 peptide (F115−Hse210). In (C) and (D) are compared spectra from labeled or unlabeled CB8 peptide (I311−H328). a.i.: arbitrary intensity.

C-terminal end, namely, the I311−K318 region (ILFGKKFK).

Posttranslational Modifications of Anc2p. The N-terminal peptide CB1, which extends from residue S2 to M29, could not be sequenced, indicating the presence of a blocked N-terminus and clearly demonstrating the absence of a Met residue at this position. Consistent with this statement, the *m*/*z* value measured by MALDI-MS for CB1 was 3054, instead of the expected value of 3010 (Table 1), showing the presence of an acetylated N-terminal Ser residue. Therefore, it is concluded that the yeast Anc2p starts with an N-acetylated N-terminal Ser and is only 317 residues long.

This result was corroborated by MALDI-MS analysis of a partially purified Anc2p sample of a HTP pass-through fraction in 0.2% EM (data not shown). A mass of 34 284 Da was determined, lower than that calculated from the DNA-deduced amino acid sequence, 34 427 Da, consistent with the absence of the N-terminal Met residue and the N-acetylation of Ser 2. However, the measured mass is 54 Da lower than expected, that is unexplained so far.

The occurrence of a posttranslational modification has been demonstrated for the beef ADP/ATP carrier, which was shown to contain a trimethyl group attached to Lys 51 (*30*). Alignment of the carrier sequences from beef and yeast (Anc2p) shows that Lys 51 corresponds to Ala 68 of Anc2p, located within the CB3 peptide. The closest Lys residue, at position 66 of Anc2p, is not modified since it is identified as phenylthiohydantoin-lysine during Edman degradation analysis. As mentioned above, the peptide CB3 displayed an intriguing behavior since during SDS−PAGE it migrated as two distinct peptides, with close apparent MW (about 6000 and 5500), but with the correct N-terminal amino acid sequence (LKQGTLDRKY). MALDI-MS analyses of tryptic digests of the two separated bands gave identical patterns. However, a partial unspecific cleavage at the C-terminal end of CB3 cannot be excluded. At the present time, no clear data explain the behavior of the CB3 peptide.

DISCUSSION

This paper reports on the synthesis of a novel photoactivatable analogue of ADP, 2-azido-N-[^{32}P]ADP, and on its use to map the substrate binding sites of the yeast mitochondrial ADP/ATP carrier. To avoid misinterpretation of results, our study has been carried out on the Anc2p isoform of the yeast ADP/ATP carrier present in mitochondria from a genetically modified *S. cerevisiae* strain carrying disrupted *ANC1* and *ANC3* genes (*27*, *31*).

To identify the binding site(s) of this substrate analogue, Anc2p was photolabeled in the mitochondrial membrane, and then purified and subjected to chemical fragmentation. The resulting peptides were separated by SDS−PAGE and microsequenced or were analyzed by MALDI and ESI mass spectrometry approaches which require highly purified Anc2p. Since HTP-purified carrier preparations contain several contaminant proteins and a large amount of ergosterol (*27*), we used in the present study a His-tagged carrier, Anc2-(His$_6$)p, purified by affinity chromatography on Ni−NTA resin (*14*).

Specific Binding of 2-Azido-N-[^{32}P]ADP to Anc2p in Mitochondria. Previous studies performed in our laboratory have reported that, in the absence of photoirradiation, 2-azido-ADP interacts specifically and reversibly with the membrane-embedded beef heart ADP/ATP carrier (*6*). Upon

photoactivation, 2-azido-ADP was covalently attached to the carrier, thus allowing mapping of the substrate binding sites. In contrast to the report by Mayinger et al. (*7*), attempts to investigate the ADP binding sites of the yeast mitochondrial ADP/ATP carrier, using a similar approach, failed because of an unexpected enzymatic cleavage of the [β-^{32}P]phosphate group of the probe. This problem was totally overcome by introduction of a naphthoyl group at the 3′ position of the ribose moiety of 2-azido-ADP. The resulting 2-azido-N-[^{32}P]-ADP displayed no detectable degradation upon incubation with yeast mitochondria. The criteria of specificity and affinity required for binding of a photoactivatable ligand to a receptor are fulfilled in the case of 2-azido-N-[^{32}P] ADP since, when assayed in darkness, the photoprobe could bind with high affinity ($K_d \sim 3$ μM) to Anc2p in mitochondria, the specificity of the binding being demonstrated by CATR displacement. This finding was not surprising since, as previously reported, 3′-*O*-N-ADP interacts with high affinity with the ADP/ATP carrier, either in the membrane-bound state or when isolated in detergent solution (*32*, *33*). Finally, similarly to both 2-azido-ADP and 3′-*O*-N-ADP (*6*, *26*), 2-azido-N-[^{32}P]ADP is not transported into mitochondria.

Upon photoirradiation of yeast mitochondria in the presence of 2-azido-N-[^{32}P]ADP, only Anc2p or Anc2(His$_6$)p was covalently labeled, as assessed by the fact that the presence of CATR totally prevented any photolabeling. This preliminary result demonstrated the high specificity of incorporation of 2-azido-N-[^{32}P]ADP that was a prerequisite for undoubted identification of Anc2p nucleotide binding domains.

Photolabeling of Anc2p and Anc2(His$_6$)p with 2-Azido-N-[^{32}P]ADP. Distribution of radioactivity on fragments generated by CNBr cleavage of 2-azido-N-[^{32}P]ADP-photolabeled Anc2p or Anc2(His$_6$)p demonstrated clearly that two regions of the polypeptide chain were photolabeled. A precise localization of incorporation of the probe has been achieved by microsequencing and MALDI mass spectrometry applied to the labeled peptides.

Binding sites were assigned to the central part, S183−R191, and to the C-terminal region, I311−K318. As 2-azido-N-[^{32}P]ADP is not transported into yeast mitochondria, it is concluded that the two regions were accessible to the photoprobe from the cytosol. These findings are consistent with the previous identification by our group of two regions of the beef heart ADP/ATP carrier specifically photolabeled by the nontransportable 2-azido-ADP, located in the central and in the C-terminal parts (*6*). In contrast, Mayinger et al. (*7*) reported the photolabeling by azido-[^{32}P]ATP of only one large central binding region, G172−M210, in the wild-type yeast ADP/ATP carrier, consistent with their proposal of a single reorientating site model for nucleotide transport. Puzzling enough, in their experiments, high MW peptides resulting from incomplete CNBr cleavage of the photolabeled carrier were not ^{32}P-labeled, though comprising the G172−M210 peptide. Photolabeling of the S183−R191 segment of the carrier, as demonstrated in the present study, is in agreement with that of the G172−M210 region, but photolabeling of the C-terminal segment of the carrier (this study) was not detected in (*7*). This discrepancy may originate from inappropriate experimental conditions used in the latter work during handling of the photolabeled material. We have previously reported that low MW peptides could be washed out of the acrylamide gel during the staining−destaining process (*6*), thus leading to possible misinterpretation of mapping results.

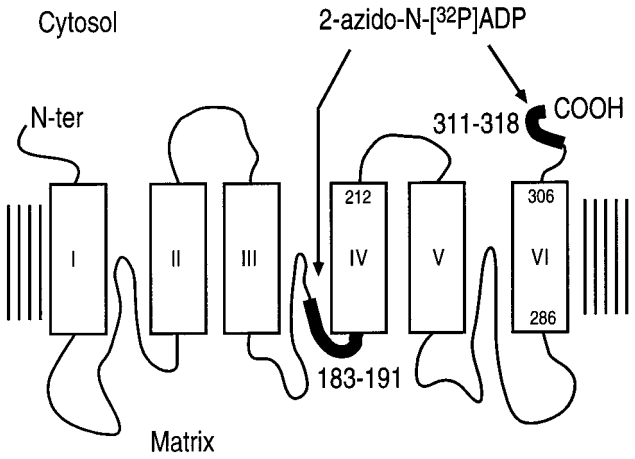

FIGURE 7: Schematic representation of the postulated arrangement of the yeast ADP/ATP carrier monomer in the mitochondrial membrane, according to (*34*), based on the presence of six transmembrane helices (I−VI). The two regions labeled by 2-azido-N-[^{32}P]ADP, identified in this paper as S183−R191 and I311−K318, are indicated as heavy black lines.

From our results, the presence of two distinct ADP binding regions is obvious in the two ADP/ATP carriers examined so far and therefore is highly significant with respect to folding of the peptide chain and nucleotide recognition and transport.

The two photolabeled regions of the ADP/ATP carrier identified in the present study are shorter than those previously reported (*6*, *7*), thus allowing a more precise localization of regions of the carrier involved in nucleotide binding. Figure 7 shows their location within a possible arrangement of the carrier in the mitochondrial membrane, based on the 3-fold symmetry of the carrier and on hydropathy plots (*34*). This model postulates six amphiphilic helices that cross the membrane and are connected through more hydrophilic loops. The N-terminal and C-terminal regions have been demonstrated to be exposed to the cytosol (*13*, *35*, *36*). Other models of the ADP/ATP carrier have been proposed (*37*−*40*). They differ from one to another with respect to the folding of the connecting loops, which are viewed either as protruding in the extramembrane space or as inserting to various extents into the membrane, based on their reactivity to chemical reagents (*41*) or proteases (*42*). According to the model illustrated on Figure 7, photolabeled sequences of Anc2p clearly do not belong to transmembrane helices.

Specific photolabeling of Anc2p by 2-azido-N-[^{32}P]ADP results from high-affinity binding of the photoprobe and from the fact that the azido group is attached without any spacer arm to the purine ring of ADP. As a consequence, it is likely that photolabeled segments are localized within the nucleotide binding site(s). As illustrated on Figure 8, several hypotheses can be proposed to support this statement, taking into account that one nucleotide binds per carrier dimer on sites exposed to cytosol in mitochondria (*26*). (1) Photolabeled regions would belong to the same binding site within a carrier monomer. This hypothesis implies that carrier monomers of a dimer are nonequivalent, only one of them being able to bind the nucleotide, but all of the dimers are organized in a similar way (Figure 8A). (2) It can be assumed

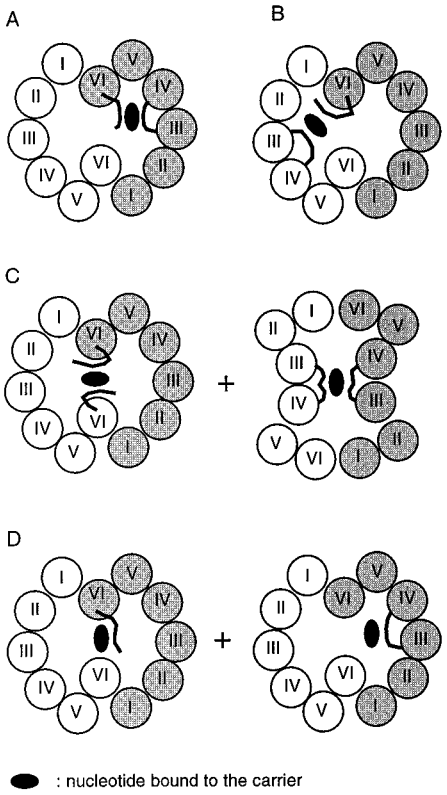

FIGURE 8: Scheme illustrating the possible organizations of Anc2p nucleotide binding sites. Top view is from the intermembrane space. The two regions photolabeled by 2-azidonaphthoyl-ADP, S183−R191 and I311−K318, are accessible from the cytoplasm. It is assumed that one nucleotide molecule is bound per carrier dimer. The postulated transmembrane helices of Anc2p monomers (numbered from I to VI) are differently colored for each monomer.

that the two labeled regions pertain to distinct carrier monomers. Binding sites resulting from the juxtaposition of the C-terminal region of one monomer and the central segment of another monomer would reflect the presence of a single family of dimers, equivalent in terms of nucleotide binding site organization (Figure 8B). (3) Alternatively, either two C-terminal regions or two central regions of distinct monomers would form two types of binding sites (Figure 8C). Because of the binding stoichiometry (one nucleotide per carrier dimer), this implies repartition of carrier dimers into two different families and excludes sites made by juxtaposition of two C-terminal and two central regions within the same dimer. (4) Photolabeled segments are not juxtaposed but belong to distinct dimers which are therefore distributed in two families (Figure 8D). As a consequence, the existence of two classes of structurally different binding sites and that of monomers displaying different conformations within the carrier dimers is assumed.

Finally, these hypotheses can accommodate previous demonstrations of two types of cytosolic ADP binding sites on the carrier in mitochondria, considering a possible tetrameric organization of the transport unit (*26*).

Whereas plausible, the proximity of regions S183−R191 and I311−K318 deserves some comments in terms of structural considerations, since the ADP/ATP carrier is inserted asymmetrically in the mitochondrial membrane (*13*). Sidedness of the photolabeled segments is ensured since (1) only membrane-embedded carrier was used and (2) 2-azido-N-[^{32}P]ADP was not transported into mitochondria. According to the arrangement of the carrier presented in Figure 7, the labeled C-terminal region is freely accessible to the probe added from the cytosol, whereas the S183−R191 region, directly linked to a transmembrane α-helix, belongs to a hairpin-shaped loop partially inserted in the bilayer. This suggests that the cytosolic C-terminal region is flexible enough to bend within the membrane toward the S183−R191 matrix segment, in a hydrophilic environment, since its mobility is not impaired by the presence of a His-tag extension at its C-terminal extremity. It might be proposed that 2-azido-N-[^{32}P]ADP, although not transported, follows the same way and penetrates to some extent into the protein prior to binding. Transport cannot be triggered probably because of the steric hindrance due to the presence of azido and naphthoyl groups. A similar situation has been reported concerning the uncoupling protein (UCP), in which externally added photoactivatable ATP analogue-labeled peptidic segments are located in the C-terminal third of UCP and exposed to the matrix compartment (*43*).

Work is in progress to define the involvement of the two nucleotide binding regions of the ADP/ATP carrier in the transport process, using site-directed mutagenesis to identify strategic residues and genetic engineering to remove the C-terminal end of the carrier. Further studies will be extended to the exploration of the carrier nucleotide binding sites accessible from the matrix compartment.

ACKNOWLEDGMENT

We thank Mathilde Louwagie for expert amino acid sequencing

REFERENCES

1. Ward, D. G., and Cavieres, J. D. (1998) *J. Biol. Chem. 273*, 33759−33765.
2. McIntosh, D. B., Woolley, D. G., MacLennan, D. H., Vilsen, B., and Andersen, J. P. (1999) *J. Biol. Chem. 274*, 25227−25236.
3. Hipfner, D. R., Deeley, R. G., and Cole, S. P. (1999) *Biochim. Biophys. Acta 1461*, 359−376.
4. MacLeod, K. J., Vasilyeva, E., Merdek, K., Vogel, P. D., and Forgac, M. (1999) *J. Biol. Chem. 274*, 32869−32874.
5. Boulay, F., Lauquin, G. J.-M., Tsugita, A., and Vignais, P. V. (1983) *Biochemistry 22*, 477−484.
6. Dalbon, P., Brandolin, G., Boulay, F., Hoppe, J., and Vignais, P. V. (1988) *Biochemistry 27*, 5141−5149.
7. Mayinger, P., Winkler, E., and Klingenberg, M. (1989) *FEBS Lett. 244*, 421−426.
8. Brandolin, G., Le Saux, A., Trézéguet, V., Vignais, P. V., and Lauquin, G. J.-M. (1993) *Biochem. Biophys. Res. Commun. 192*, 143−150.
9. Ashani, Y., and Catravas, G. N. (1980) *Anal. Biochem. 109*, 55−62.
10. Laemmli, U. K. (1970) *Nature 227*, 680−685.
11. Schägger, H., and von Jagow, G. (1987) *Anal. Biochem. 166*, 368−379.
12. Towbin, H., Staehelin, T., and Gordon, J. (1979) *Proc. Natl. Acad. Sci. U.S.A. 76*, 4350−4354.
13. Brandolin, G., Boulay, F., Dalbon, P., and Vignais, P. V. (1989) *Biochemistry 28*, 1093−1100.
14. Fiore C., Trézéguet, V., Roux, P., Le Saux, A., Noël, F., Schwimmer, C., Arlot, D., Dianoux, A. C., Lauquin, G. J.-M., and Brandolin, G. (2000) *Protein Expression Purif. 19*, 57−65.
15. Daum, G., Bohni, P. C., and Schatz, G. (1982) *J. Biol. Chem. 257*, 13028−13033.
16. Krämer, R., and Klingenberg, M. (1979) *Biochemistry 18*, 4209−4215.

17. Boulay, F., Dalbon, P., and Vignais, P. V. (1985) *Biochemistry 24*, 7372−7379.
18. Sowa, T., and Ouchi, S. (1975) *Bull. Chem. Soc. Jpn. 48*, 2084−2090.
19. Schäfer, G., and Onur, G. (1980) *FEBS Lett. 109*, 197−201.
20. Gottikh, B. P., Krayevsky, A. A., Tarussova, N. B., Purygin, P. P., and Tsilevich, T. L. (1970) *Tetrahedron 26*, 4419−4433.
21. Hoard, D. E., and Ott, D. G. (1965) *J. Am. Chem. Soc. 87*, 1785−1788.
22. Bornstein, P. (1969) *Biochem. Biophys. Res. Commun. 36*, 957−964.
23. Gross, E., and Witkop, B. (1961) *J. Am. Chem. Soc. 83*, 1510−1511.
24. Rabilloud, T., Kieffer, S., Procaccio, V., Louwagie, M., Courchesne, P. L., Patterson, S. D., Martinez, P., Garin, J., and Lunardi, J. (1998) *Electrophoresis 19*, 1006−1014.
25. Schlimme, E., Boos, K. S., and de Groot, E. J. (1980) *Biochemistry 19*, 5569−5574.
26. Block, M. R., and Vignais, P. V. (1984) *Biochim. Biophys. Acta 767*, 369−376.
27. Le Saux, A., Roux, P., Trézéguet, V., Fiore, C., Schwimmer, C., Dianoux, A. C., Vignais, P. V., Brandolin, G., and Lauquin, G. J.-M. (1996) *Biochemistry 35*, 16116−16124.
28. Porath, J., and Olin, B. (1983) *Biochemistry 22*, 1621−1630.
29. Jaquinod, M. (1993) Thesis, Université Louis Pasteur, Strasbourg.
30. Klingenberg, M. (1985) *The ADP/ATP carrier in mitochondrial membranes* (Martonosi, A., Ed.) Vol. 4, Plenum Publishing Corporation, New York.
31. Roux, P., Le Saux, A., Trézéguet, V., Fiore, C., Schwimmer, C., Dianoux, A. C., Vignais, P. V., Lauquin, G. J.-M., and Brandolin, G. (1996) *Biochemistry 35*, 16125−16131.
32. Block, M. R., Lauquin, G. J.-M., and Vignais, P. V. (1982) *Biochemistry 21*, 5451−5457.
33. Dupont, Y., Brandolin, G., and Vignais, P. V. (1982) *Biochemistry 21*, 6343−6347.
34. Walker, J. E., and Runswick, M. J. (1993) *J. Bioenerg. Biomembr. 25*, 435−446.
35. Trézéguet, V., Le Saux, A., David, C., Gourdet, C., Fiore, C., Dianoux, A. C., Brandolin, G., and Lauquin, G. J.-M. (2000) *Biochim. Biophys. Acta 1457*, 81−93.
36. Hatanaka, T., Hashimoto, M., Majima, E., Shinohara, Y., and Terada, H. (1999) *Biochem. Biophys. Res. Commun. 262*, 726−730.
37. Brandolin, G., Le Saux, A., Trézéguet, V., Lauquin, G. J.-M., and Vignais, P. V. (1993) *J. Bioenerg. Biomembr. 25*, 459−472.
38. Klingenberg, M. (1993) *J. Bioenerg. Biomembr. 25*, 447−457.
39. Nelson, D. R., Lawson, J. E., Klingenberg, M., and Douglas, M. G. (1993) *J. Mol. Biol. 230*, 1159−1170.
40. Klingenberg, M., and Nelson, D. R. (1994) *Biochim. Biophys. Acta 1187*, 241−244.
41. Bogner, W., Aquila, H., and Klingenberg, M. (1986) *Eur. J. Biochem. 161*, 611−620.
42. Marty, I., Brandolin, G., Gagnon, J., Brasseur, R., and Vignais, P. V. (1992) *Biochemistry 31*, 4058−4065.
43. Mayinger, P., and Klingenberg, M. (1992) *Biochemistry 31*, 10536−10543.

BI000618L